

CONF-9605173--16
ANL/ASD/CP-89598

Design and Commissioning of the Photon Monitors and Optical Transport Lines for the Advanced Photon Source Positron Accumulator Ring*

W. Berg, B. Yang, A. Lumpkin, and J. Jones

*Advanced Photon Source, Argonne National Laboratory
9700 South Cass Avenue, Argonne, IL 60439*

RECEIVED
NOV 21 1996
OSTI

Abstract. Two photon monitors have been designed and installed in the positron accumulator ring (PAR) of the Advanced Photon Source. The photon monitors characterize the beam's transverse profile, bunch length, emittance, and energy spread in a nonintrusive manner. An optical transport line delivers synchrotron light from the PAR out of a high radiation environment. Both charge-coupled device and fast-gated, intensified cameras are used to measure the transverse beam profile (0.11-1 mm for damped beam) with a resolution of 0.06 mm. A streak camera ($\sigma_t = 1$ ps) is used to measure the bunch length which is in the range of 0.3-1 ns. The design of the various transport components and commissioning results of the photon monitors will be discussed.

INTRODUCTION

MASTER

The Advanced Photon Source (APS) positron accumulator ring is designed to be filled by a 450-MeV positron linac at 60 Hz (1). The positron accumulator ring (PAR) is 30.667 meters in circumference and operates with a fundamental frequency of 9.776 MHz. However, the addition of power at the 12th harmonic (117 MHz) produces further compression resulting in a shorter bunch for efficient injection into the booster synchrotron. High field dipoles (1.48 Tesla) are used to bend the positron beam around the ring (2). Synchrotron light emitted from the source points within the dipoles allow measurement of the transverse beam size, bunch length, emittance, and energy spread via the photon monitors.

PHOTON MONITOR TRANSPORT LINES

Two optical transport lines have been designed and installed in order to deliver synchrotron light out of the machine's high radiation environment into a user-safe

* Work supported by U. S. Department of Energy, Office of Basic Energy Sciences under Contract No. W-31-109-ENG-38.

DISTRIBUTION OF THIS DOCUMENT IS UNLIMITED

The submitted manuscript has been authored by a contractor of the U. S. Government under contract No. W-31-109-ENG-38. Accordingly, the U. S. Government retains a nonexclusive, royalty-free license to publish or reproduce the published form of this contribution, or allow others to do so, for U. S. Government purposes.

DISCLAIMER

This report was prepared as an account of work sponsored by an agency of the United States Government. Neither the United States Government nor any agency thereof, nor any of their employees, makes any warranty, express or implied, or assumes any legal liability or responsibility for the accuracy, completeness, or usefulness of any information, apparatus, product, or process disclosed, or represents that its use would not infringe privately owned rights. Reference herein to any specific commercial product, process, or service by trade name, trademark, manufacturer, or otherwise does not necessarily constitute or imply its endorsement, recommendation, or favoring by the United States Government or any agency thereof. The views and opinions of authors expressed herein do not necessarily state or reflect those of the United States Government or any agency thereof.

DISCLAIMER

Portions of this document may be illegible in electronic image products. Images are produced from the best available original document.

area. Some of the key considerations for the design were light transport efficiency, vibration, and reduction of air/thermal turbulence. Evacuated vacuum chambers, which house the optical components, are used to reduce the effect of air currents. The transport system overview is shown in Fig. 1(a). Figure 1(b) shows a diagram

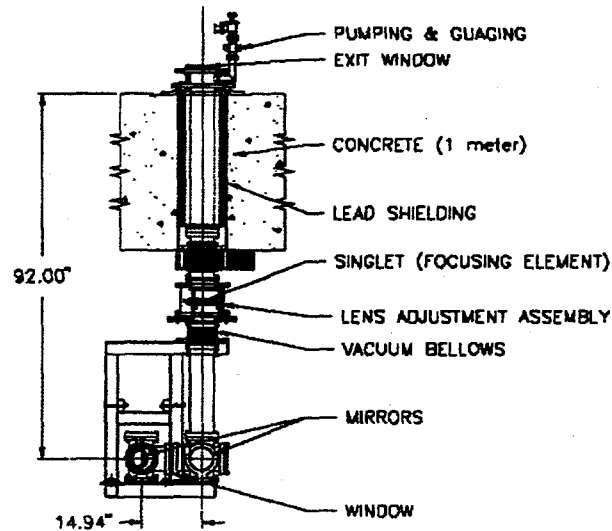


FIGURE 1a. Transport line components.

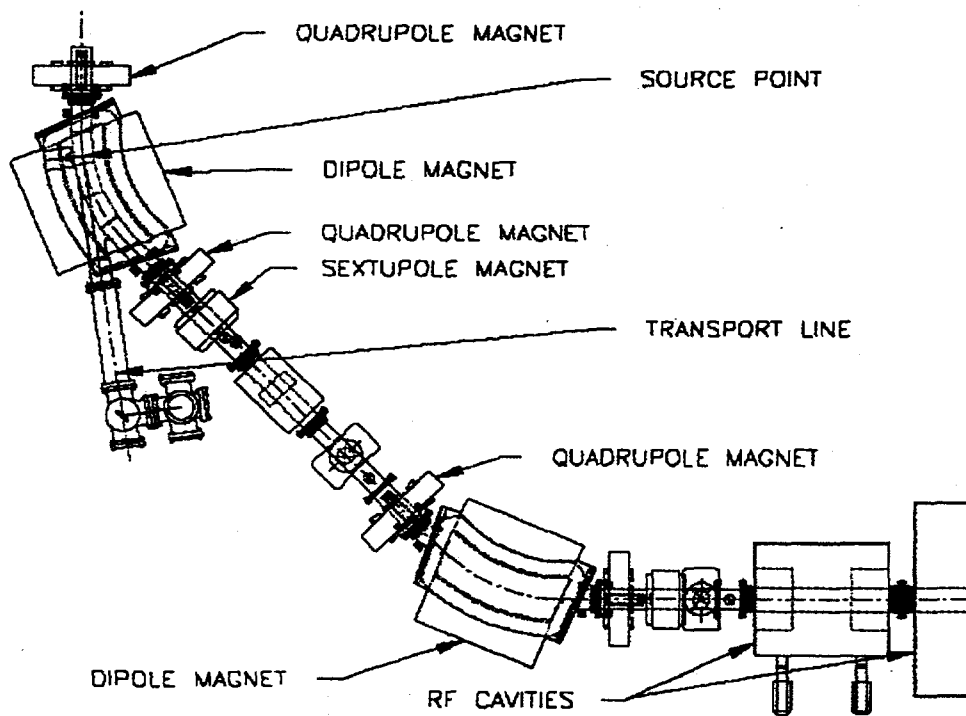


FIGURE 1b. One quadrant of the PAR showing the location of the source point.

of a typical source point located in a dipole vacuum chamber. A retractable fiducial target inserted at the source point will provide a reference to verify the system alignment, focus, resolution, and magnification.

The main imaging component of the transport line is a double convex quartz lens. The lens projects an image to the center of the optics table where the cameras are mounted. Table 1 shows the design parameters of the transport system. The performance of the transport optics were modeled using the commercial ray-tracing program ZEMAX (3). The results are given in Table 2.

TABLE 1. Design Parameters for the Transport Line

| | |
|--------------------------|-----------------|
| Lens material / diameter | quartz / 150 mm |
| Focal length | 1.65 m |
| Distance from the source | 3.00 m |
| Distance from the image | 3.67 m |
| Magnification | 1.22 |

TABLE 2. Spatial Resolution for the Transport Line
($\lambda=532$ nm, $\Delta\lambda=10$ nm, 8 mrad horizontal acceptance)

| | |
|---|--------------------|
| Diffraction contribution | 14 μ m |
| Depth of source contribution | 5 μ m |
| Geometric and chromatic aberration | 12 μ m |
| Imperfect optics distortion (estimated) | 12 μ m |
| Combined resolution | 23 μ m |
| Beam size | 600 - 1110 μ m |

The visible synchrotron light from the source point is intercepted by a 4" moly mirror (radiation cooled). The light is reflected through a quartz window which isolates the ring from the transport system. This isolation enables adjustment and maintenance of the optics without venting the ring. A number of quartz mirrors direct the light through a fused silica lens to an optics table. Considerable effort was put into design and selection of components for a vacuum-compatible lens adjustment housing. The lens can be adjusted with three degrees of freedom for final alignment.

The x-ray shielding specifications required that a significant amount of lead be placed in and around the transport penetrations that were cast into the concrete. A 1.5" thick lead sleeve poured between two steel tubes with support flanges welded to the ends provide the bulk of the shielding. The lead liner, pictured in Fig. 2, shows the lead as it is being installed into a penetration. Vibration isolation pads located under the supporting base of the exit vacuum chamber help reduce the low-frequency vibrations generated from nearby machinery. Soft bellows were incorporated into the transport line on either side of the lens housing to reduce vibration



FIGURE 2. Installation of lead shielding.

transfer from the mezzanine floor above the ring. The light exits the transport vacuum chamber through a quartz window and is directed onto an optics table for imaging. Several views of the finished installation are shown in Figs. 3(a), (b), and (c).

CAMERAS AND IMAGING RESULTS

A gated, intensified camera (Stanford Computer Optics: Quik05) was placed at the focal point of the transport system to readout beam images (4). The fast gate (minimum of 5 ns) allows the acquisition of beam images in a single turn/single pass. Such capability is useful in studying transient phenomena at the time of injection, extraction, and compression (turn-on of 12th harmonic power).

Two charge-coupled device (CCD) cameras with secondary optics provide routine observation of the beam. Since the two photon ports have very different dispersions, the transverse beam profile data for stored beam yields information on both beam emittance and energy spread. The images from the above cameras are combined with a video quad (American Dynamics AD1476) for routine viewing by the machine operators (5). Table 3 lists the measured beam profile and Fig. 4 shows a typical image and the transverse beam profiles.

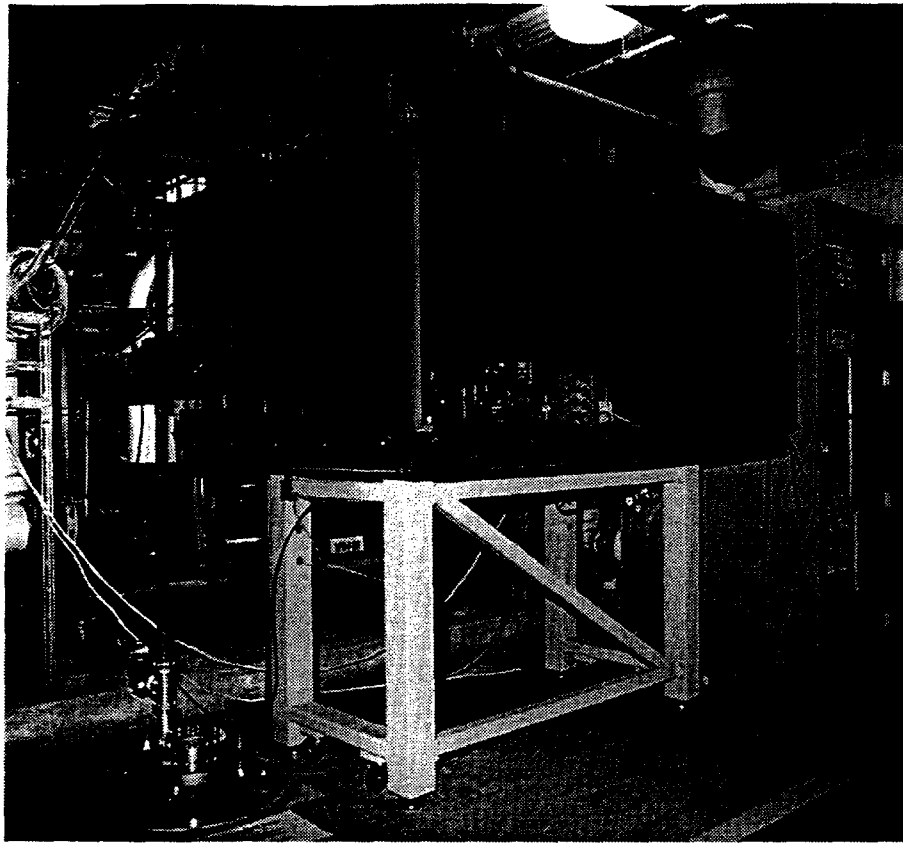


FIGURE 3a. Exit window and optics table.

TABLE 3. Lattice Function and Measured Beam Profiles (RF12 off)

| Direction | x | | y | | |
|-------------------|------|-------|-------|-------|-------|
| | Port | No. 1 | No. 2 | No. 1 | No. 2 |
| Beta function (m) | | 4.1 | 3.2 | 13.5 | 3.4 |
| Dispersion (m) | | 0.0 | -2.6 | 0.0 | 0.0 |
| Beam size (mm) | | 0.91 | 1.01 | 0.18 | 0.11 |

A streak camera is used to observe the bunch length. Figure 5(a) is a streak image which shows the effect of the bunch compression on stored beam. After the 12th harmonic power is turned on, the bunch starts to lengthen from 0.8 ns but eventually damps down to 0.3 ns (Fig. 5(b)). The damping time constant is deduced from the progressive changes of the profiles. Table 4 summarizes the measured beam parameters which compare favorably with the design values. The longer bunch lengths are due to the lower rf voltage used (17 kV applied vs 30 kV designed) during these measurements.

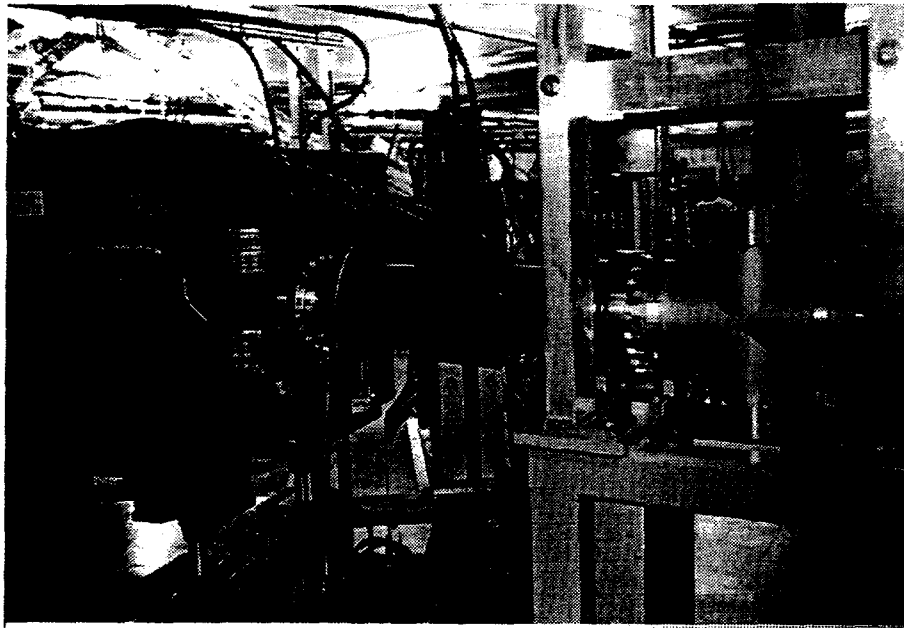


FIGURE 3b. Source point transport section.

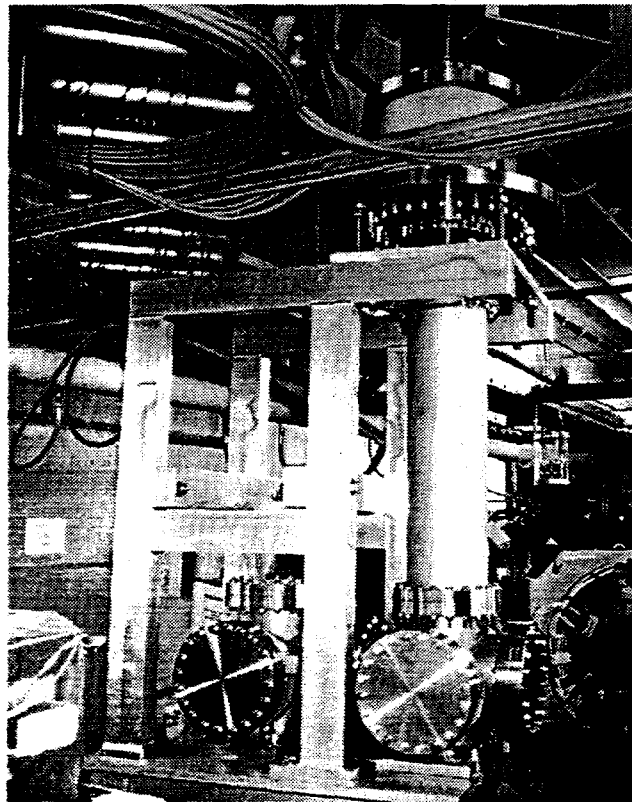


FIGURE 3c. Transport and lens housing.

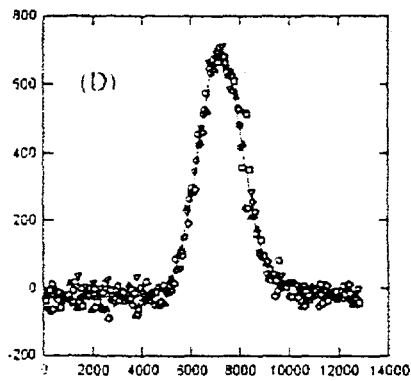
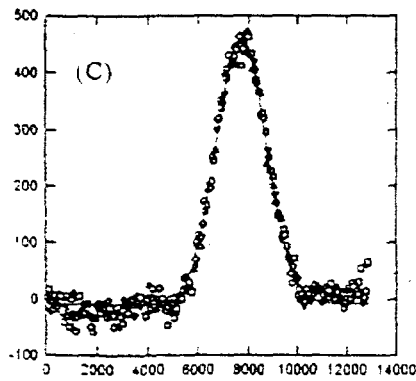
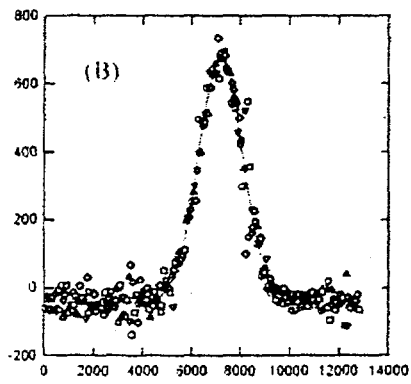
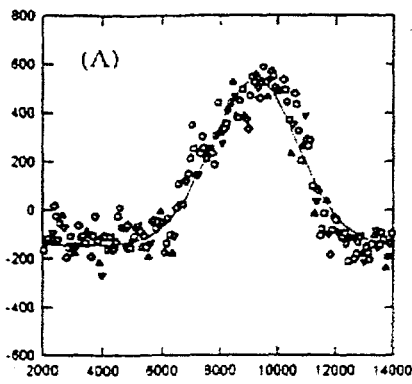


FIGURE 4. Top: Typical images as viewed from quad display.
Bottom: Typical plot profiles, Intensity vs. Size (μm).

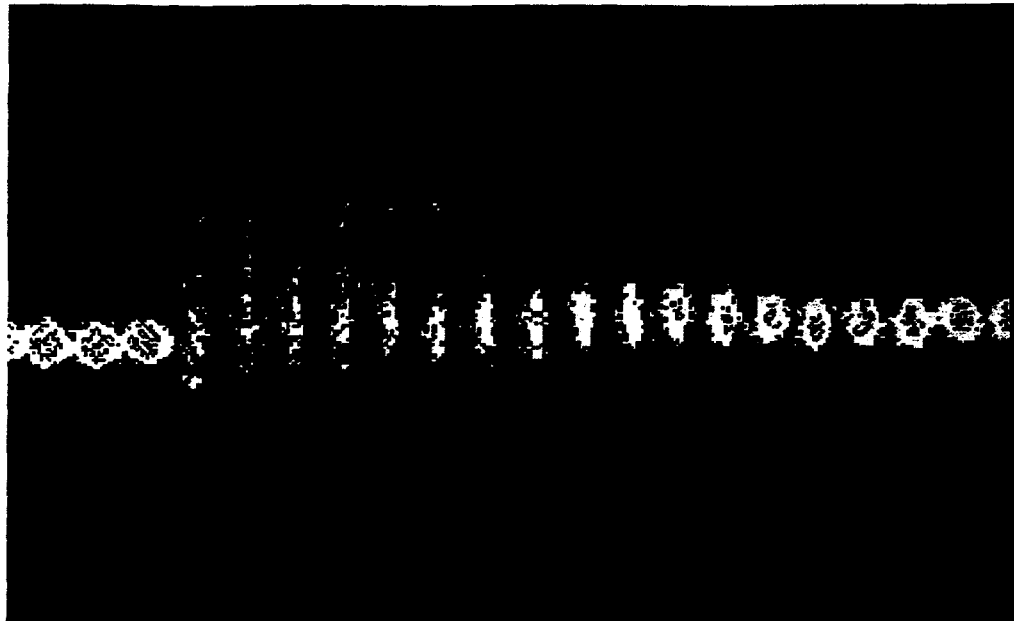


FIGURE 5a. Dual sweep streak image with 12th harmonic turned on. The vertical span of the image is 10 ns and the horizontal is 50 ms. The vertical streak was triggered every 2 ms.

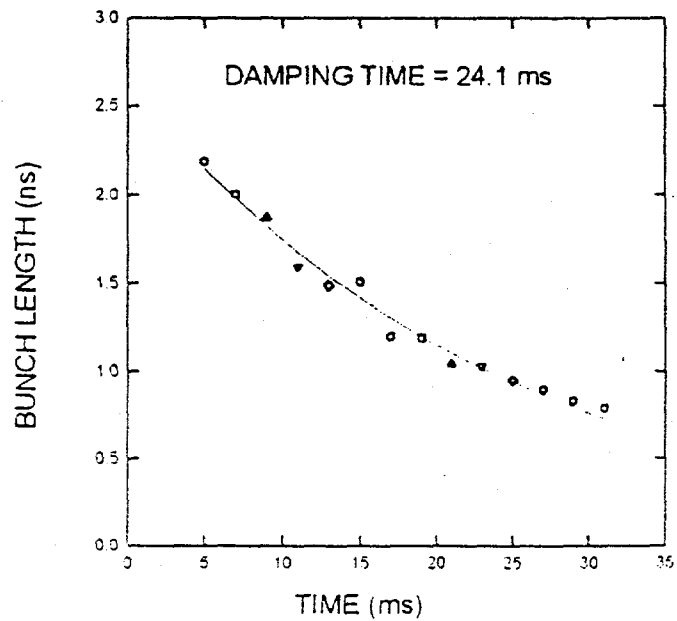


FIGURE 5b. Bunch length as a function of time demonstrating the damping effects with 12th harmonic applied.

TABLE 4. Transverse and Longitudinal Beam Profiles (E=375 MeV)

| Quantity | Measured | Design (6) |
|---------------------------|----------------------|----------------------|
| Emittance (mm·mrad) | | |
| e_x | 0.20 | 0.25 |
| e_y | 0.0024 | < 0.025 |
| Vertical coupling | 0.012 | < 0.1 |
| Energy spread | 2.5×10^{-3} | 2.8×10^{-3} |
| Bunch length | | |
| RF12 off | 0.84 ns | 0.67 ns |
| RF12 on | 0.31 ns | 0.21 ns |
| Longitudinal damping time | | |
| RF12 on | 24.1 ms | 25.4 ms |

CONCLUSION

There are now two transport lines installed in the PAR, and commissioning of the photon monitors is underway. Initial measurements of the emittance, vertical coupling, bunch length, and longitudinal damping time have been performed. The results are found to be consistent with the design objectives. Further refinement and integration of the photon monitors into the APS control system is in progress.

ACKNOWLEDGMENTS

The authors would like to acknowledge the extra efforts put in by CAD designers Dave Fallin and Anatoly Oberfeld. Without their special attention to detail and nurturing of this project installation efforts would have been much more painful, to say the least. Also many thanks go to Mike Borland for his advice and, more importantly, his patience.

REFERENCES

1. A. Lumpkin et al., "Initial Diagnostics Commissioning Results for the Advanced Photon Source (APS)." Proceedings of the 1995 Particle Accelerator Conference, Dallas, Texas, May 1-5, 1995, pp. 2473-2475 (1996).
2. Annex to 7-GeV Advanced Photon Source Conceptual Design Report, ANL-87-15 Annex, p. II. 10-10, May 1988.
3. Focussoft Inc., ZEMAX Optical Design Program, Pleasanton, CA.
4. Stanford Computer Optics, Palo Alto, CA.
5. American Dynamics, Orangeburg, NY.
6. M. Borland, private communication.